DOI: 10.2478/sspjce-2024-0009

A Proposal for a Simplified Mesoscale Simulation Model of a Reinforced Concrete Frame with and without Masonry Infill

Karim Benyahi[1*], Amar Messas[1]

[1] Laboratoire de Modélisation des Matériaux et Structures en Génie Civil (L2MSGC), Faculté du Génie de la Construction, Université Mouloud Mammeri de Tizi Ouzou, 15000 Tizi-ouzou, Algeria
*e-mail: karim.benyahi@ummto.dz

Abstract

This article proposes a simplified micro-modeling of masonry infill walls, as well as a method for modeling reinforced concrete frames without infill. This model uses the Drucker-Prager criterion to simulate the non-linear compression behavior of bricks. And for the frame elements, the concrete damaged plasticity (CDP) model was used. This numerical modeling strategy is characterized by the absence of discrete elements either at the portal frame level, or at the masonry unit level, the latter often used to simulate the onset of damage in areas susceptible to plasticization. This model was checked against experimental results and analytical solutions. Subsequently, the use of the concrete damaged plasticity (CDP) model to simulate the non-linear behavior of bricks demonstrated the model's ability to simulate and reproduce experimental damage.

Keywords: numerical modelling, meso-scale model, masonry infilled frames, collapse resistance

1 Introduction

For a long time, the masonry wall was considered as a non-structural element, neglected during the design of the reinforced concrete (RC) frame structures, these have been considered solely for their thermal and sound insulation properties. It was only after the occurrence of the various earthquakes that the post-seismic reports showed their importance and influence. As a result, the study of the behavior of these structures, as well as their simulation, has become a key subject in earthquake engineering.

Frame structures with infill exhibit complex behavior; on one side we have a frame which exhibits a flexible but ductile behavior, and on the other a masonry wall which exhibits a rigid but fragile behavior. The introduction of the masonry walls to the frame increases considerably the rigidity of the structure, greater than the sum of the member stiffness taken individually, this increase is due to the interaction between the frame and the filling wall. This increase in stiffness has a direct impact on the structure, this has the effect of reducing the period of the structure (El-Ouali et al., 1991 [1]). Among other things, an increase in seismic forces can be observed [2] (Wakabayashi, 1986). Many experimental and analytical studies have been carried out on frame structures.

Murty and Jain (2000) [3] conducted an experimental study on the influence of masonry on frame structures, the results show that infill walls increase the strength, stiffness, and overall energy dissipation of the structure. Dawe and Seah (1989) [4] conducted experimental studies on steel frames with concrete infill, the study looked at the influence of many parameters on the behavior and resistance of infilled frame structures subjected to horizontal loading. Crisafulli (1997) [5] carried out experimental tests, with the aim of setting up a capacity dimensioning method for frames with infill. The author recommends the introduction of diagonal frames at each of the frame nodes, with "U" bars linked to the longitudinal reinforcement, allowing a better transfer of the lateral forces from the frame to the infill panel. Yuen and Kuang (2012) [6] conducted an analytical study on the seismic behavior of framed structures with infill under dynamic loading in-plane and out-of-plane. Chrysostomou (1991) [7] during a dynamic analytical study, observes a clear reduction in the bending moments as well as the shear force in the elements of the infilled frame structures in comparison with the elements of the frame without infill. He also observes a considerable increase in the normal forces in the members of the infilled frame structures in comparison with the members of the frame without infill.

Through years of research, many authors have focused on the study of these structures and their modeling has become widespread, especially with the arrival of the finite element method. Many authors have looked into the modeling of infill walls, proposing many strategies over time. The authors D'Altri et al. (2019) [8], Ali and Page (1988) [9] report that in the history of masonry modeling, Page (1978) [10] was the first to consider the masonry units as well as the mortar separately, in this first attempt the bricks are elastic elements acting in conjunction with connecting elements simulating mortar joints. Ali and Page (1988) [9] subsequently proposed a modeling of masonry walls by finite elements subjected to a loading in plan, the bricks and mortar joints are modeled separately. In this method, failure can occur by crushing or cracking of the constituents, or by failure of the bond at the brick-mortar interface. Lotfi and Shing (1994) [11] propose a constitutive model capable of simulating fracture initiation and propagation under combined normal and shear stresses. The model is of the meso-modeling type where the mortar units are modeled with continuous elements, the mortar joints are modeled by interface elements. Lourenço and Rots (1994) [12]; Lourenço and Rots (1997) [13] propose an interface model that takes into account all types of masonry failure, the bricks are modeled by continuous elements, and the mortar joints by interface elements. The damage is then concentrated in the mortar joints and potential cracking elements are introduced into the center of the masonry units. Lourenço and Rots (1997) [13] based on the approach of Lourenço and Rots (1994) [12], the author proposes a simplified micro modeling approach where the damage is concentrated in the mortar joints, through interface elements that replace the different mortar joints, potential cracks are introduced into masonry units through interface elements. Aref and Dolatshahi (2013) [14] offer a simplified micro-modelling, the model allows the simulation of filling walls subjected to a three-dimensional loading, monotonic or cyclic. The mortar joints are replaced by zero-thickness interface elements; a constitutive material model was subsequently introduced through a subroutine in Abaqus software. The brick elements are modeled by solid elements (C3D8R) and the interface elements by plane elements (C0H3D8). The authors introduced the cyclic behavior of masonry, using the model proposed by Lourenço and Rots

(1997) [13]. Nasiri and Liu (2017) [15] propose a simplified modeling of the infill in order to take into account the out-of-plane loading. The model was established by replacing the mortar joints with zero-thickness interface elements, the masonry units are connected and interact with each other through these interface elements. Kuang and Yuen (2013) [16] propose an approach based on the surface-based interaction modeling technique to simulate the interfacial ten-sile-separation behavior between the contact surfaces of masonry units. Bolhassani et al. (2015) [17] offer experimental tests for determining the mechanical characteristics of masonry elements, as well as their numerical simulation using micro-simplified modelling. Abdulla et al. (2017) [18] propose a simplified micro-modeling method by introducing the extended finite element method (XFEM). The method allows simulation of in-plane and out-of-plane infill walls for monotonic or cyclic loading. Zhai et al. (2017) [19] propose the use of discrete elements in order to circumvent one of the limitations of the diffuse crack model which is the dependence of the solution on the size of the mesh, relying on the element method finite extended (XFEM), the author introduces discrete elements in the frame and the masonry units in order to simulate the possible cracks of the latter. D'Altri et al. (2018) [20] proposed a detailed micro-modeling model for masonry structures, the model allows the prediction of the mechanical behavior of these structures until their failure.

The aim of this paper is to propose a method for modeling reinforced concrete frames without infill, with the commercial software Abaqus, using the appropriate behavior laws for concrete and steel. Then, in a second step, the introduction of the infill wall according to the appropriate plastic model, enables the global behavior of a reinforced concrete frame with infill to be modeled through the use of a trial-and-error method to calibrate the analytical model on the experimental model. As this method can be classified as a simplified micro-modeling of reinforced concrete frames with infill, while bypassing the use of discrete elements, it presents by its simplicity an easy and accessible alternative to the complex models present in the literature.

2 Materials and methods

The nonlinear behavior of the concrete can be simulated according to various models in the literature, it can be simulated by using the theory of plasticity or damage models, the theory of plasticity makes it possible to describe the irreversible deformations, the damage model is al-lowing to describe the gradual degradation of the initial rigidity. For a better simulation of the non-linear behavior of concrete, the coupling between the models of plasticity and damage is essential (Nguyen and Korsunsky, 2008 [21]).

In this paper, the non-linear behavior of concrete will be simulated with the CDP (Concrete Damaged Plasticity) model integrated in Abaqus, this model is based on the formulation of Lubliner et al. (1989) [22] and Lee and Fenves (1998) [23], makes it possible to represent in a complete way the plastic behavior of the concrete, by taking into account its damage. The model assumes a non-associated plastic flow potential, the flow function used for this model is the Drucker-Prager hyperbolic function.

2.1 Concrete

According to the methodology proposed by Alfarah et al. (2017) [24], the behavior of concrete in compression goes through three stages (see Figure 1(a)), two ascending segments and another descending one, the ascending segments in compression follow the recommendations of CEB-FIP (2010) [25] and the descending segment follow the recommendation of Krätzig and Pölling (2004) [26].

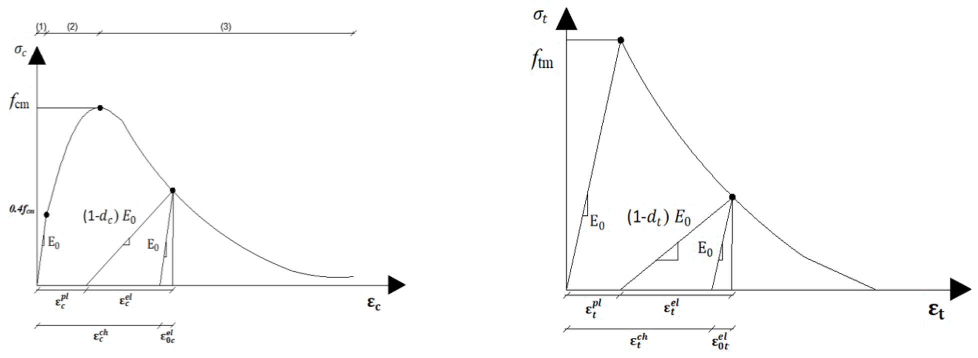

(a) (b)

Figure 1: Compressive and tensile behavior of concrete: (a) Compression, (b) Tension

The first is linear elastic, it is expressed by the following relation:

$$\sigma_c = E_0 \varepsilon_C \tag{1}$$

The second follows a quadratic law, which is expressed by:

$$\sigma_c = \frac{E_{ci}\dfrac{\varepsilon_{ci}}{f_{cm}} - \left(\dfrac{\varepsilon_c}{\varepsilon_{cm}}\right)^2}{1+\left(E_{ci}\dfrac{\varepsilon_c}{f_{cm}} - 2\right)\dfrac{\varepsilon_c}{\varepsilon_{cm}}} f_{cm} \tag{2}$$

$$E_{ci} = 10000\left(f_{cm}\right)^{1/3} \tag{3}$$

$$E_0 = \left(0.8 + 0.2\left(\frac{f_{cm}}{88}\right)\right)E_{ci} \tag{4}$$

$$f_{cm} = f_{ck} + 8 \tag{5}$$

The third is a downward curve, which is expressed by:

$$\sigma_c = \left(\frac{2+\gamma_c f_{cm}\varepsilon_{cm}}{2f_{cm}} - \gamma_c\varepsilon_c + \frac{\varepsilon_c^2\gamma_c}{2\varepsilon_{cm}}\right)^{-1} \tag{6}$$

$$\gamma_c = \frac{\pi^2 f_{cm}\varepsilon_{cm}}{2\left[\frac{G_{ch}}{l_{eq}} - 0.5f_{cm}\left(\varepsilon_{cm}(1-b) + b\frac{f_{cm}}{E_0}\right)\right]^2} \tag{7}$$

$$b = \frac{\varepsilon_c^{pl}}{\varepsilon_c^{ch}} \tag{8}$$

The tension curve follows two segments:

A first linear elastic, it is expressed by the following relation:

$$\sigma_t = E_0\varepsilon_t \tag{9}$$

A second segment that follows the law:

$$\sigma_t = \left[\left[1+\left(c_1\frac{w}{w_c}\right)^3\right]e^{-c_2\frac{w}{w_c}} - \frac{w}{w_c}\left(1+c_1^3\right)e^{-c_2}\right]f_{tm} \tag{10}$$

$$f_{tm} = 0.3016\left(f_{ck}\right)^{2/3} \tag{11}$$

With:
C_1= 3 and C_2=6.93 according to the values recommended by Alfarah et al. (2017) [24].

$$w_c = 5.14\left(\frac{G_f}{f_{tm}}\right) \tag{12}$$

$$G_f = 0.073\left(f_{cm}\right)^{0.18} \tag{13}$$

$$G_{ch} = \left(\frac{f_{cm}}{f_{tm}}\right)^2 G_f \tag{14}$$

Equation (10) can be written in terms of tensile strain using the following equation:

$$\varepsilon_t = \varepsilon_{tm} + \left(\frac{w}{l_{eq}}\right) \tag{15}$$

The damage model proposed by Alfarah et al. (2017) [24] was also used to calculate the concrete damage variable, a program under Fortran following the methodology recommended by the authors was written for this purpose.

The strain relationship of the concrete damaged plasticity (CDP) model (Figure 1) is expressed as follows:

$$\varepsilon = \varepsilon^{el} + \varepsilon^{pl} \tag{16}$$

The stress-strain relationship, taking into account the isotropic damage parameter, can be expressed as follows:

$$\sigma = (1-d)D_0^{el}:(\varepsilon - \varepsilon^{pl}) = D^{el}:(\varepsilon - \varepsilon^{pl}) \tag{17}$$

The expression for the load function is given by:

$$F(\overline{\sigma}, \tilde{\varepsilon}^{pl}) \leq 0 \tag{18}$$

The flow law is expressed as follows:

$$\dot{\varepsilon}^{pl} = \dot{\lambda}\frac{\partial G(\overline{\sigma})}{\partial(\overline{\sigma})} \tag{19}$$

When the concrete sample is unloaded, resulting in a drop in material stiffness (Figure 1), the latter is characterized by two damage variables d_c and d_t, expressed as follows:

$$d_t = d_t(\tilde{\varepsilon}^{pl}) \ and \ 0 \leq d_t \leq 1 \tag{20}$$

$$d_c = d_c(\tilde{\varepsilon}^{pl}) \ and \ 0 \leq d_c \leq 1 \tag{21}$$

The stress-strain relationship under tensile and compressive loading, taking into account the damage variables d_c and d_t, can be expressed as follows:

$$\sigma_t = (1-d_t)E_0(\varepsilon_t - \tilde{\varepsilon}_t^{pl}) \tag{22}$$

$$\sigma_c = (1-d_c)\ E_0(\varepsilon_c - \tilde{\varepsilon}_c^{pl}) \tag{23}$$

The effective tensile and uniaxial compressive stresses resulting from crack propagation are then given as follows:

$$\tilde{\sigma}_t = \frac{\sigma_t}{(1-d_t)} = E_0(\varepsilon_t - \tilde{\varepsilon}_t^{pl}) \tag{24}$$

$$\tilde{\sigma}_c = \frac{\sigma_c}{(1-d_c)} = E_0(\varepsilon_c - \tilde{\varepsilon}_c^{pl}) \tag{25}$$

The inelastic stress-strain curves to be used in the modelling are given as follows:

$$\tilde{\varepsilon}_c^{in} = \varepsilon - \frac{\sigma_c}{E_0} \tag{26}$$

$$\tilde{\varepsilon}_c^{pl} = \tilde{\varepsilon}_c^{in} - \frac{d_c}{(1-d_c)}\frac{\sigma_c}{E_0} \tag{27}$$

$$\tilde{\varepsilon}_t^{pl} = \tilde{\varepsilon}_t^{ck} - \frac{d_t}{(1-d_t)}\frac{\sigma_t}{E_0} \tag{28}$$

2.2 Rebar steel

The rebar steel is modeled with an elastoplastic behavior with isotropic hardening (Figure 2). The stress is described by the following BAEL99 (1999) [27]:

$$\sigma = \begin{cases} E_a \,.\, \varepsilon & \text{for} \quad 0 \leq \varepsilon_r < \varepsilon_e \\ \sigma_e & \text{for} \quad \varepsilon_e \leq \varepsilon \leq \varepsilon_u \\ 0 & \text{for} \quad \varepsilon > \varepsilon_u \end{cases} \tag{29}$$

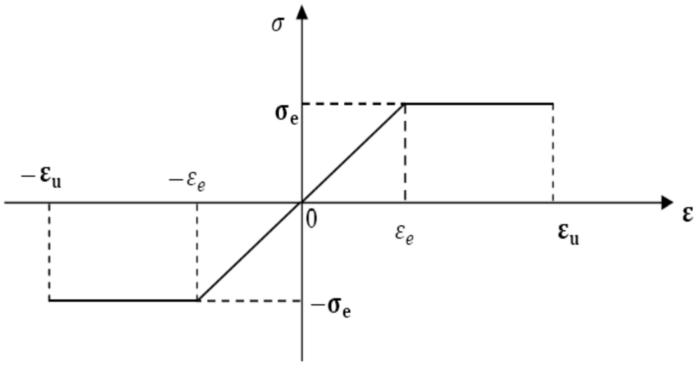

Figure 2: Perfect elastoplastic law of a reinforced concrete steel according to BAEL99 [27]

3 Nonlinear Behavior Modeling of Concrete Masonry Units

In this method, the simulation of the nonlinear behavior of the concrete masonry units can be represented by two models, the CDP model or by using the Drucker-Prager plastic model. In this paper, the Drucker-Prager model will be mainly used for experimental validation and the CDP model for masonry unit will be discussed later.

3.1 Drucker Prager Model

For materials with internal friction, such as sands, soils, rocks and concrete, it is not possible to neglect the effect of the first invariant I1 in the yield condition (Jirasek and Bazant, 2001 [28]). The first effective criterion written in terms of I1 and J2 was proposed by Burzyński (1929) [29] according to Jirasek and Bazant (2001) [28]. Later, Drucker and Prager (1952) [30] will propose his model, and his criterion is usually stated as follows:

$$f\left(I_1, J_2\right) \equiv \alpha I_1 + \sqrt{J_2} - \tau_0 \tag{30}$$

α and τ_0 are the material parameters, I_1 and J_2 are respectively the first invariant and the second deviatoric invariant. This model has been widely used, particularly in the modeling of confined concrete Oh (2003) [31]; Karabinis and Kiousis (1994) [32]. Later, many authors will propose modifications to this model (Yu et al., 2010 [33]; Zhang et al., 2015 [34]; Mohammadi et al., 2019 [35]), in this article the extended Drucker-Prager model will be used to simulate the non-linear behavior of bricks in compression.

Three yield criteria with different shapes of yield surfaces in the meridian plane (p-t plane) can be used in this model: a linear form, a hyperbolic form and a general exponent form. In our case the linear form was chosen, according to the recommendation of Yu et al. (2010) [33], which recommends the use of a criterion taking into account the third deviatoric invariant, as well as a function of yield non-circular.

The yield criteria in a linear form is expressed as Abaqus (2011) [36]:

$$F = t - \tan\beta - d = 0 \tag{31}$$

$$t = \frac{1}{2}q\left[1 + \frac{1}{K} - \left(1 - \frac{1}{K}\right)\left(\frac{r}{q}\right)^3\right] \tag{32}$$

With:

$$q = \sqrt{3J_2} \tag{33}$$

$$J_2 = \frac{1}{2}s : s = \frac{1}{2}s_{i.j}s_{i.j} = \frac{1}{6}\left[\left(\sigma_1 - \sigma_2\right)^2 + \left(\sigma_2 - \sigma_3\right)^2 + \left(\sigma_3 - \sigma_1\right)^2\right] \tag{34}$$

In this paper, hardening is defined by the elastic compressive stress, we will have:

$$d = \left(1 - \frac{1}{3}tan\beta\right)\sigma_c \tag{35}$$

3.2 Modeling of the Connection Between the Concrete Masonry Units

Usually the connection between the different concrete masonry units is represented by a cohesive relationship of the traction-separation type.
After failure of the cohesive bond, Coulomb's law is applied to express the friction between the different concrete masonry units.

In the case of a frame with infill, this same connection is applied between the frame and the masonry. In our case, the connection between the different concrete masonry units will be modeled in this way. The contact between the different surfaces of the concrete masonry units is expressed through two types of behavior included in Abaqus software. The first is "hard contact behavior" which supposes a transmission of stresses for the surfaces in contact. It minimizes the penetration of the slave surface in the master surface at stress locations and does not allow tensile stress transfer across the interface (Abaqus, 2011 [36]). The second is tangential where a coefficient of friction will be determined by groping to simulate the behavior of the concrete masonry units in contact with each other. As for the connection between the reinforced concrete (RC) frame and the concrete masonry units, it will be done using the "Tie" module included in Abaqus explicit.

This type of contact has been used to model confined masonry in the past by Borah et al. (2021) [37]; Chandel and Sreevalli (2019) [38]; Okail et al. (2016) [39]. In this paper, its use will be generalized for classical masonry. Furthermore, the model proposed here, offers a slight improvement by taking into account the masonry units separately, this makes it possible to take into account the mode of failure by horizontal slip of the bed joints of the masonry.

One of the limits of the proposed model is the dependence of the solution on the size of the mesh, as mentioned by Borah et al. (2021) [37], the mesh size must be calibrated in order to have the numerical solution close to the experimental solution.

4 Results and discussion

The experimental test of Mehrabi and Shing (1994) [41] shown in Figure 3, this test consists of a progressive thrust until the failure of a reinforced concrete (RC) frame with masonry infills. The reinforced concrete (RC) frame being the same as that which was validated during the first part.

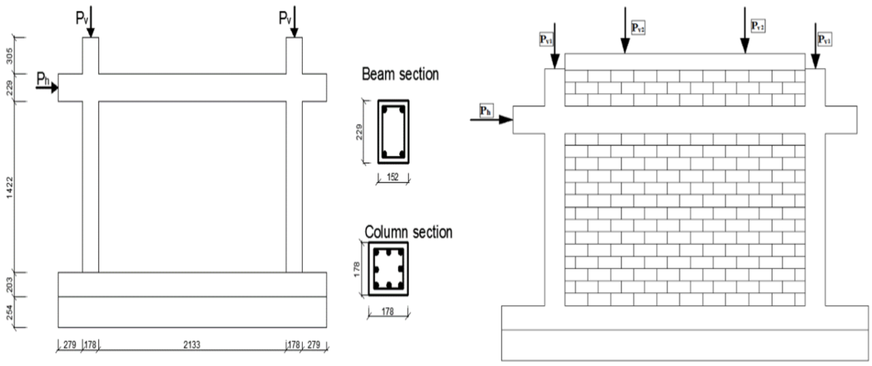

Figure 3: Experimental model of the reinforced concrete (RC) frame with masonry infill

The mechanical characteristics of concrete and steel reinforcement are given in Table 1 and 2.

Table 1: Mechanical characteristics of concrete

E_c (MPa)	f_{c28} (MPa)	f_{t28} (MPa)
21930	30.9	3.29

Table 2: Mechanical characteristics of steel reinforcement

Type of reinforcement	E_S (MPa)	f_y (MPa)	f_u (MPa)
Longitudinal	195000	420.7	662.1
Transverse	195000	367.6	449.6

Even though the masonry units are perforated units, in our model they are represented as complete units with the following dimensions: 204 x 102 x 102 mm. This simplification was used by Bolhassani et al. (2015) [17] and showed satisfactory results.

Even though the masonry units are perforated units (Fig. 15), in our model they are represented as complete units with the following dimensions: 204 x 102 x 102 mm. This simplification was used by Bolhassani et al. (2015) [17] and showed satisfactory results. Fig. 15 shows the dimensions of the masonry units used during the experimental test by Mehrabi and Shing (1994) [41].

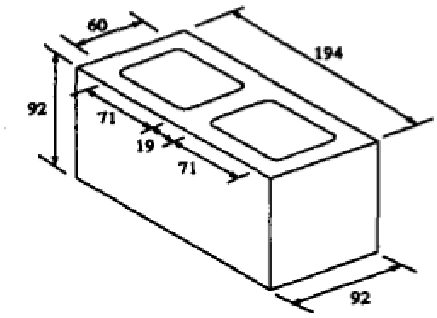

Fig. 15 Concrete masonry units of the experimental test (Mehrabi and Shing, 1994 [41])

The following Tables summarize the different parameters assigned when modeling concrete masonry units in Abaqus.

Table 3: Values assigned for the mechanical behavior of concrete masonry units

Parameters	ν	E (MPa)	fc (MPa)
Values	0.15	15400	16.48

The different parameters assigned when modeling concrete masonry units in Abaqus follow Drucker Prager model with: R of 1, ψ of 27 and β of 2.

The experimental test conducted by Mehrabi and Shing (1994) [41] consists of imposing two loads were imposed on the frame along the analysis, first a fixed vertical load with a value of 293 kN; distributed between the columns (195.4 kN) and the beam (97.6 kN), and another laterally incremented monotonic load, applied according to the controlled displacement mode. The vertical load was applied first and was kept constant until the frame collapsed.

4.1 Results of the Reinforced Concrete (RC) Frame without Masonry Infill

Figure 4 shows a comparison between the analytical results with those of the experimental test conducted by Mehrabi and Shing (1994) [41], from the curves we can see that our numerical model describes in a suitable way the behavior of the frame, we can even see that the elastic behavior is obtained in a more specific way than the numerical model of Mehrabi and Shing (1997) [40], this demonstrates the robustness of the proposed model. The agreement of the ultimate load between experience and our calculation is satisfactory; a slight overestimation of the ultimate load can be seen towards the end.

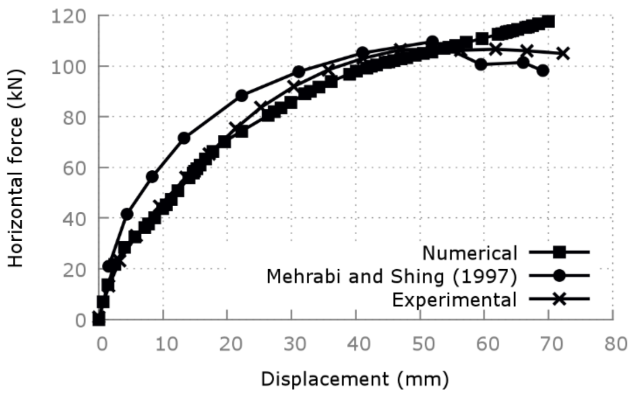

Figure 4: Load-displacement curves for the RC frame without masonry infill

In the elastic part, the experimental test conducted by Mehrabi and Shing (1994) [41] has an initial stiffness of 474.77 N/mm; in comparison, the numerical model presented by this study presents an initial stiffness of 463.22 N/mm, for the numerical model of Mehrabi and Shing (1997) [40] the latter is 675.63 N/mm. The numerical model presents a difference in terms of initial stiffness of 2.43%, for the numerical model of Mehrabi and Shing (1997) [40], this difference is 20.9 %.

Table 3: Comparison between initial stiffness's

Frame without masonry infill	Ultimate load P_u (kN)	Error (%)	Initial stiffness (N/mm)	Error (%)
Experimental	106.62	-	4747.7	-
Numerical	117.47	10.17	4632.2	2.43
Mehrabi and Shing (1997)	108.65	1.90	6756.2	20.9

The results in Table 3 indicate an ultimate experimental load of 106.62 kN and that obtained by our calculation of 117.47 kN, i.e. a difference of about 10.17 %.
Our numerical model presents an average error estimated at 4.83% of the experimental load, that of Mehrabi and Shing (1997) [40] presents an average error estimated at 9.1% of the experimental load. This demonstrates that our numerical model manages to simulate the plastic behavior of the experimental curve more adequately than that of Mehrabi and Shing (1997) [40].

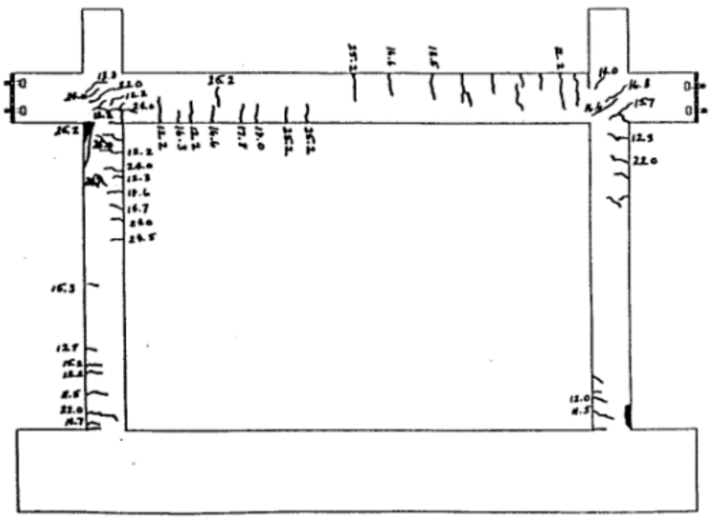

(a)

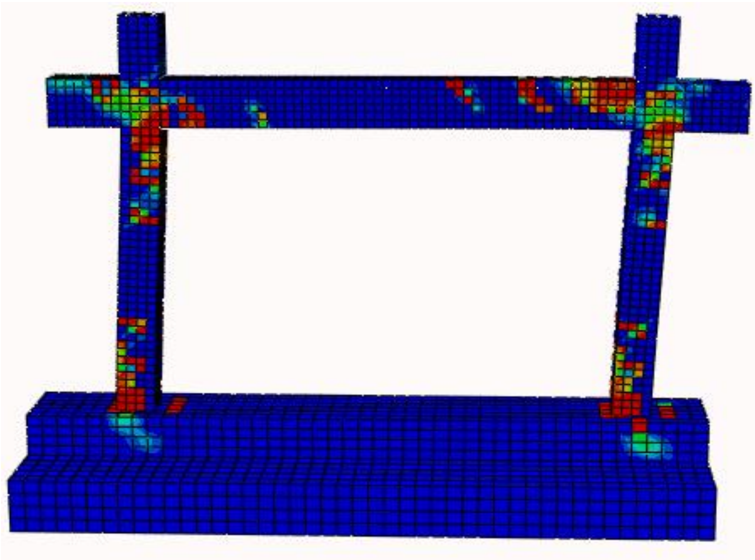

(b)

Figure 5: Damage evolution of the reinforced concrete (RC) bare frame: (a) Experimental test (Mehrabi and Shing, 1994 [41]), (b) Numerical study

By comparing the damage in Figure 5(a) which shows the level of damage suffered by the reinforced concrete (RC) frame during the experimental test, the damage given by the numerical model (Figure (5b)) succeeds in reproducing the damaged zones well, especially in the nodal and tense zones, we can therefore conclude that the damage model proposed by Alfarah et al. (2017) [24] is perfectly suited for modeling the damage of reinforced concrete.

4.2 Results of the Reinforced Concrete (RC) Frame with Masonry Infill

Figure 6 shows a comparison between the experimental and numerical model, where we can see an acceptable similarity of the proposed model.

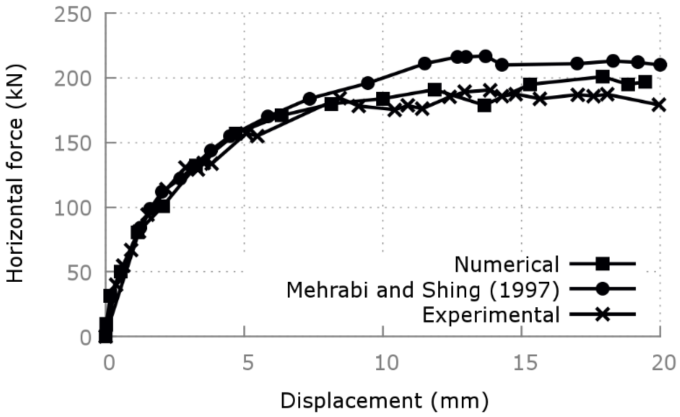

Figure 6: Load-displacement curves for the RC frame with masonry infill

The ultimate experimental load of 190 kN and the ultimate load obtained by our calculation of 201 kN. The agreement between the ultimate load found by our calculation and that measured is satisfactory. Our model overestimates the ultimate load by about 5.78%.

It can be seen that our simulation and that of Mehrabi and Shing (1997) [40] give an appearance close to the experimental curve. However, the two curves obtained differ at the level of the ultimate load, where our calculation seems to approach the experimental better than the simulation carried out by Mehrabi and Shing (1997) [40].

From Figure (6), it can be also seen that the Drucker-Prager model more accurately describes the behavior of the frame with masonry infill than the Concrete Damage Plasticity (CDP) model. The ultimate experimental load of 190 kN, and the ultimate load obtained by the Drucker-Prager model of 201 kN, and that obtained by the Concrete Damage plasticity (CDP) model is 208 kN. The agreement between the ultimate load found by the Concrete Damage Plasticity (CDP) model and that measured is satisfactory. The Concrete Damage Plasticity (CDP) model overestimates the ultimate load by about 9.47% compared to the experimental.

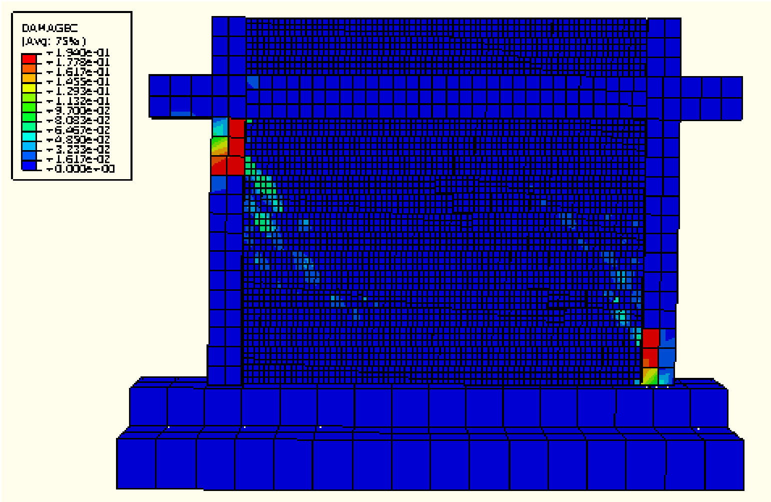
DAMAGEC
(Avg: 75%)
+1.940e-01
+1.778e-01
+1.617e-01
+1.455e-01
+1.293e-01
+1.132e-01
+9.700e-02
+8.083e-02
+6.467e-02
+4.850e-02
+3.233e-02
+1.617e-02
+0.000e+00

(a)

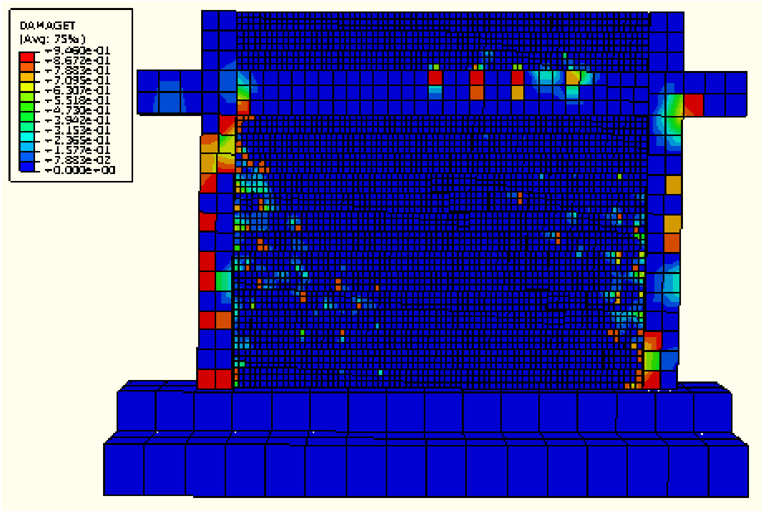
DAMAGET
(Avg: 75%)
+9.460e-01
+8.672e-01
+7.883e-01
+7.095e-01
+6.307e-01
+5.518e-01
+4.730e-01
+3.942e-01
+3.153e-01
+2.365e-01
+1.577e-01
+7.883e-02
+0.000e+00

(b)

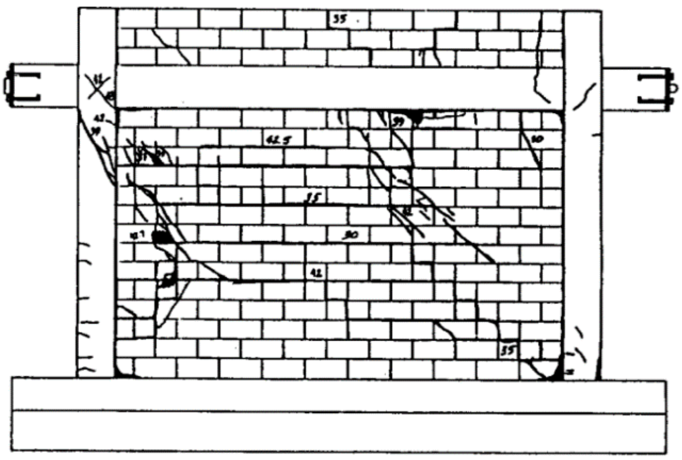

(c)

Figure 7: Numerical and experimental damage evolution of the RC frame with masonry infill: (a) Compression damage, (b) Tension damage, (c) Experimental damage

The use of the Concrete Damage Plasticity (CDP) model makes it possible to obtain a numerical damage, the results obtained are in Figure (7a) for the damage in compression and Figure (8b) for the damage in tension.

By comparing the results obtained numerically in Figure (7a) and Figure (7b) with those obtained experimentally in Figure (7c), we can see that our model manages to reproduce the experimental damage in an acceptable way. Here the mode of failure of the infilled frame by crushing of the corners as well as the diagonal cracking could be reproduced.

5 Conclusion

In this article a modeling method for reinforced concrete (RC) frames with the Abaqus computer code, with and without masonry infill, has been introduced. At first, the use of a damage model present in the literature, added to the various modules integrated in Abaqus allows us to model the damage in a reinforced concrete (RC) frame structure.

The introduction of discrete elements is the most widespread method to simulate the behavior between the concrete masonry units in contact, as well as the damage likely to appear in the frame or in the masonry units, this method often requires the use of relatively complex subroutines. This paper proposes an alternative to this by proposing a simplified micro-modeling which makes it possible to simulate the behavior of a reinforced concrete (RC) structure with masonry infill.

The results obtained from our numerical modeling relating to the frame with and without masonry infill are very close to the analytical and experimental results. Which allows us to say that the adopted simplified micro-modeling allows us to simulate in a correct way the nonlinear behavior of the reinforced concrete (RC) frames with and without masonry infill until the rupture.

List of notations

E_0	Elastic modulus corresponding to 0.4 of the characteristic resistance of concrete
ε_c	Strain of concrete in compression
f_{cm}	Compressive strength of concrete
f_{ck}	Characteristic value of concrete strength
ε_{cm}	Strain corresponding to the maximum strength of the concrete
G_{ch}	Concrete crushing energy
l_{eq}	Characteristic length which corresponds to mesh of the element
ε_c^{pl}	Plastic strain due to element damage
ε_c^{ch}	Concrete crushing strain
ε	Total strain

ε^{el} Elastic strain
σ Elastic stress
d The damage variable
D_0^{el} The elastic stiffness matrix
D^{el} The deteriorated stiffness matrix
$\bar{\sigma}$ Effective stress
$\tilde{\varepsilon}^{pl}$ Equivalent plastic strain
$\dot{\lambda}$ Not-negative multiplier
$\tilde{\varepsilon}_t^{pl}$ Equivalent plastic strains in tension
$\tilde{\varepsilon}_c^{pl}$ Equivalent plastic strains in compression

References

[1] El-Ouali, T., Houde, J., Tinawi, R. (1991). Comportement d'un cadre rempli soumis à un chargement cyclique : modélisation pour une analyse dynamique non linéaire. *Canadian Journal of Civil Engineering*. 18(6), pp. 1013-1023. https://doi.org/10.1139/l91-124

[2] Wakabayashi, M. (1986). Design of earthquake-resistant buildings. McGraw-Hill Companies

[3] Murty, C.V.R., Jain, S.K. (2000). Beneficial influence of masonry infill walls on seismic performance of RC frame buildings. In 12th world conference on earthquake engineering

[4] Dawe, J., Seah, C.K. (1989). Behaviour of masonry infilled steel frames. *Canadian Journal of Civil Engineering.* 16(6), pp. 865-876. https://doi.org/10.1139/l89-129

[5] Crisafulli, F.J. (1997). Seismic behaviour of reinforced concrete structures with masonry infills. Doctoral dissertation, University of Canterbury

[6] Yuen, Y.P., Kuang, J.S. (2012). Nonlinear response and failure mechanism of infilled RC frame structures under biaxial seismic excitation. In Proceedings of the 15th World Conference on Earthquake Engineering, Lisboa, Portugal

[7] Chrysostomou, C.Z. (1991). Effects of degrading infill walls on the nonlinear seismic response of two-dimensional steel frames. Doctoral dissertation, Cornell University

[8] D'Altri, A.M., Sarhosis, V., Milani, G., Rots, J., Cattari, S., Lagomarsino, S., Sacco, E., Tralli, A., Castellazzi, G., de Miranda, S. (2019). Modeling strategies for the computational analysis of unreinforced masonry structures: review and classification. *Archives of computational methods in engineering*, pp. 1-33. https://doi.org/10.1007/s11831-019-09351-x

[9] Ali, S.S., Page, A.W. (1988). Finite element model for masonry subjected to concentrated loads. *Journal of structural engineering.* 114(8), pp. 1761-1784. https://doi.org/10.1061/(ASCE)0733-9445(1988)114:8(1761)

[10] Page, A.W. (1978). Finite element model for masonry. *Journal of the Structural Division.* 104(8), pp 1267-1285. https://doi.org/10.1061/JSDEAG.0004969

[11] Lotfi, H.R., Shing, P.B. (1994). Interface model applied to fracture of masonry structures. *Journal of structural engineering.* 120(1), pp. 63-80. https://doi.org/10.1061/(ASCE)0733-9445(1994)120:1(63)

[12] Lourenço, P.B., Rots, J. (1994). Analysis of masonry structures with interface elements. Rep. No. 03-21-22-0, 1

[13] Lourenço, P.B., Rots, J.G. (1997). Multisurface interface model for analysis of masonry structures. *Journal of engineering mechanics*. 123(7), pp. 660-668. https://doi.org/10.1061/(ASCE)0733-9399(1997)123:7(660)

[14] Aref, A.J., Dolatshahi, K.M. (2013). A three-dimensional cyclic meso-scale numerical procedure for simulation of unreinforced masonry structures. Computers & Structures. 120, pp. 9-23. https://doi.org/10.1016/j.compstruc.2013.01.012

[15] Nasiri, E., Liu, Y. (2017). Development of a detailed 3D FE model for analysis of the in-plane behaviour of masonry infilled concrete frames. *Engineering Structures*. 143, pp. 603-616. https://doi.org/10.1016/j.engstruct.2017.04.049

[16] Kuang, J.S., Yuen, Y.P. (2013). Simulations of masonry-infilled reinforced concrete frame failure. *Proceedings of the Institution of Civil Engineers-Engineering and Computational Mechanics*. 166(4), pp. 179-193. https://doi.org/10.1680/eacm.13.00002

[17] Bolhassani, M., Hamid, A.A., Lau, A.C., Moon, F. (2015). Simplified micro modeling of partially grouted masonry assemblages. *Construction and Building Materials*. 83, pp. 159-173. https://doi.org/10.1016/j.conbuildmat.2015.03.021

[18] Abdulla, K.F., Cunningham, L.S., Gillie, M. (2017). Simulating masonry wall behaviour using a simplified micro-model approach. *Engineering Structures*. 151, pp. 349-365. https://doi.org/10.1016/j.engstruct.2017.08.021

[19] Zhai, C., Wang, X., Kong, J., Li, S., Xie, L. (2017). Numerical simulation of masonry-infilled RC frames using XFEM. *Journal of Structural Engineering*. 143(10), pp. 04017144. https://doi.org/10.1061/(asce)st.1943-541x.0001886

[20] D'Altri, A.M., de Miranda, S., Castellazzi, G., Sarhosis, V. (2018). A 3D detailed micro-model for the in-plane and out-of-plane numerical analysis of masonry panels. *Computers & Structures*. 206, pp. 18-30. https://doi.org/10.1016/j.compstruc.2018.06.007

[21] Nguyen, G.D., Korsunsky, A.M. (2008). Development of an approach to constitutive modelling of concrete: isotropic damage coupled with plasticity. *International Journal of Solids and Structures*. 45(20), pp. 5483-5501. https://doi.org/10.1016/j.ijsolstr.2008.05.029

[22] Lubliner, J., Oliver, J., Oller, S., Oñate, E. (1989). A plastic-damage model for concrete. *International Journal of solids and structures*. 25(3), pp. 299-326. https://doi.org/10.1016/0020-7683(89)90050-4

[23] Lee, J., Fenves, G.L. (1998). Plastic-damage model for cyclic loading of concrete structures. *Journal of engineering mechanics*. 124(8), pp. 892-900. https://doi.org/10.1061/(ASCE)0733-9399(1998)124:8(892)

[24] Alfarah, B., López-Almansa, F., Oller, S. (2017). New methodology for calculating damage variables evolution in Plastic Damage Model for RC structures. *Engineering Structures*. 132, pp. 70-86. https://doi.org/10.1016/j.engstruct.2016.11.022

[25] CEB-FIP (CEBFIP) (2010). Model code 2010. Comité euro-international du béton 594. https://doi.org/10.1007/978-3-642-41840-2_1

[26] Krätzig, W.B., Pölling, R. (2004). An elasto-plastic damage model for reinforced concrete with minimum number of material parameters. *Computers & structures*. 82(15-16), pp. 1201-1215. https://doi.org/10.1016/j.compstruc.2004.03.002

[27] Rules BAEL91 revised 99 (1999). Technical design rules and calculation of works and structures reinforced concrete according to the limit states method. Publisher: Association Francaise de Normalisation.

[28] Jirasek, M., Bazant, Z.P. (2001). Inelastic analysis of structures. John Wiley & Sons.

[29] Burzyński, W.V. (1929). Über die Anstrengungshypothesen. Schweizerische Bauzeitung. 94(21), pp. 259-262.

[30] Drucker, D.C., Prager, W. (1952). Soil mechanics and plastic analysis or limit design. *Quarterly of applied mathematics.* 10(2), pp. 157-165. https://www.jstor.org/stable/43633942

[31] Oh, B. (2003). A plasticity model for confined concrete under uniaxial loading. Doctoral dissertation, Lehigh University.

[32] Karabinis, A.I., Kiousis, P.D. (1994). Effects of confinement on concrete columns: plasticity approach. *Journal of structural engineering.* 120(9), pp. 2747-2767. https://doi.org/10.1061/(ASCE)0733-9445(1994)120:9(2747)

[33] Yu, T.T.J.G., Teng, J.G., Wong,Y.L., Dong, S.L. (2010). Finite element modeling of confined concrete-I: Drucker–Prager type plasticity model. *Engineering structures.* 32(3), pp. 665-679. https://doi.org/10.1016/j.engstruct.2009.11.014

[34] Zhang, Y., Bernhardt, M., Biscontin, G., Luo, R., Lytton, R. (2015). A generalized Drucker–Prager viscoplastic yield surface model for asphalt concrete. *Materials and Structures.* 48(11), pp. 3585-3601. https://doi.org/10.1617/s11527-014-0425-1

[35] Mohammadi, M., Dai, J.G., Wu, Y.F., Bai, Y.L. (2019). Development of extended Drucker–Prager model for non-uniform FRP-confined concrete based on triaxial tests. *Construction and Building Materials.* 224, pp. 1-18. https://doi.org/10.1016/j.conbuildmat.2019.07.061

[36] Abaqus (2011). Analysis user's manual 6.14. Dassault Systemes Simulia Corp., Providence, RI.

[37] Borah, B., Singhal, V., Kaushik, H.B. (2021). Assessment of seismic design provisions for confined masonry using experimental and numerical approaches. *Engineering Structures.* 245, pp. 112864. https://doi.org/10.1016/j.engstruct.2021.112864

[38] Chandel, V.S., Yamini Sreevalli, I. (2019). Numerical study on influence of masonry infill in an RC frame. *Asian Journal of Civil Engineering.* 20, pp. 1-8. https://doi.org/10.1007/s42107-018-0083-7

[39] Okail, H., Abdelrahman, A., Abdelkhalik, A., Metwaly, M. (2016). Experimental and analytical investigation of the lateral load response of confined masonry walls. *HBRC journal.* 12(1), pp. 33-46. https://doi.org/10.1016/j.hbrcj.2014.09.004

[40] Mehrabi, A.B., Shing, P.B. (1997). Finite element modeling of masonry-infilled RC frames. *Journal of structural engineering.* 123(5), pp. 604-613. https://doi.org/10.1061/(ASCE)0733-9445(1997)123:5(604)

[41] Mehrabi, A.B., Shing, P.B. (1994). Performance of masonry-infilled R/C frames under in-plane lateral loads: analytical modeling. In Proc., NCEER Workshop on Seismic Response of Masonry, San Francisco.